22 May 1998

ELSEVIER

Chemical Physics Letters 288 (1998) 363–370

CHEMICAL PHYSICS LETTERS

Calculation of the Raman optical activity via the sum-over-states expansion

Petr Bouř *

Institute of Organic Chemistry and Biochemistry, Academy of Sciences of the Czech Republic, Flemingovo nám. 2, Praha 6, 1660, Czech Republic

Received 27 October 1997; in final form 16 March 1998

Abstract

A new ab initio calculational method for simulations of the Raman optical activity spectra is proposed. The method is based on the sum-over-states formalism (SOS). Unlike the finite difference coupled-perturbed calculations (CP) used previously, the new scheme provides analytical derivatives of the polarization tensors and is less demanding with respect to the computer power. Although the new method is not suitable for accurate benchmark calculations, similar accuracy of the SOS and CP results was observed for the spectra of α-pinene and trans-pinane.

1. Introduction

As pointed out in previous studies [1,2], ab initio calculations are essential for correct interpretation of the vibrational optical activity measured either as the vibrational circular dichroism (VCD) or the Raman optical activity (ROA). While the ab initio modelling of VCD requires only modest increase of the computational time if compared with calculation of the force field, ROA simulations are based on a time-consuming numerical differentiation [3]. The finite difference method is clearly not appropriate for larger systems like peptides, nucleic acids or polysaccharides, spectra of which have been measured recently [3–6]. Sum-over-states (SOS) methods in conjunction with the density functional theory (DFT) were successfully used as a computationally cheaper alternative to coupled-perturbed (CP) methods for the simulations of NMR spectra [7]. Previously, we proposed an analogous excitation scheme (EXC) for calculations of polarizabilities [8] and VCD spectra [9]. Although the SOS results are not generally translationally and rotationally invariant [10], the accuracy of the calculations done on common systems was found to be comparable with the CP techniques. As shown below, this also applies for the ROA calculations, where the SOS approach is the only analytical method available.

2. Theory

General theory of the ROA phenomenon can be found elsewhere [11,12]. Here only the computation of the molecular property tensors will be discussed. For molecules the spectral response is determined by the polarizability, the optical activity tensor ($\boldsymbol{G}'$) and the dipole–quadrupole polarizability ($\boldsymbol{A}$). The polarizability can be expressed in the length ($\boldsymbol{\alpha}$) or

* Corresponding author. Fax: +420-2-2431-0503.

0009-2614/98/$19.00
PII: S0009-2614(98)00299-1

velocity ($\boldsymbol{\alpha}^v$) forms, not equal for finite precision calculations. These tensors can be written in a general notation (in atomic units, for real states):

$$T_{\alpha\beta} = \sum_{j\neq n} f_{jn}\langle n|x|j\rangle\langle j|y|n\rangle, \qquad (1)$$

where the symbols are defined as follows

$\boldsymbol{T}$	x	y	f_{jn}
$\boldsymbol{\alpha}$	μ_α	$\mu_\beta = -\sum_i r_\beta^i$	$2\omega_{jn}(\omega_{jn}^2-\omega^2)^{-1}$
$\boldsymbol{\alpha}^v$	μ_α	$\nabla_\beta = \sum_i \nabla_\beta^i$	$2(\omega_{jn}^2-\omega^2)^{-1}$
$\boldsymbol{G'}/\omega$	μ_α	$-im_\beta = -\sum_i M_\beta^i$	$-2(\omega_{jn}^2-\omega^2)^{-1}$
$\boldsymbol{A}$	μ_α	$\theta_{\beta\gamma} = \sum_i \Theta_{\beta\gamma}^i$	$2\omega_{jn}(\omega_{jn}^2-\omega^2)^{-1}$

$\boldsymbol{\nabla}$, $\boldsymbol{\mu}$, $\boldsymbol{m}$ and $\boldsymbol{\theta}$ are the gradient, electric dipole, magnetic dipole and electric quadrupole moments, respectively; $M_\beta^i = -(1/2)(\boldsymbol{r}\times\boldsymbol{\nabla})_\beta^i$ and $\Theta_{\beta\gamma}^i = -(1/2)(3r_{i\gamma}r_{i\beta} - r_i^2\delta_{\gamma\beta})$; $\boldsymbol{r}^i$ is the radius vector of an electron i. The excitation energy $\omega_{jn} = \omega_j - \omega_n$ is related to the ground (n) and an excited (j) electronic state, ω is the frequency of the incident light (corresponding to the wavelength of 514 nm for the calculations presented below, except for Table 5).

A derivative of Eq. (1) with respect to an ε-coordinate of an atom λ is

$$\begin{aligned}\left(\partial/\partial R_\varepsilon^\lambda\right)T_{\alpha\beta} = \sum_{j\neq n} f_{jn}\Big[&\left(\langle\partial n/\partial R_\varepsilon^\lambda|x|j\rangle\right.\\ &+\langle n|x|\partial j/\partial R_\varepsilon^\lambda\rangle\big)\langle j|y|n\rangle\\ &+\langle n|x|j\rangle\big(\langle\partial j/\partial R_\varepsilon^\lambda|y|n\rangle\\ &+\left.\langle j|y|\partial n/\partial R_\varepsilon^\lambda\rangle\right)\Big]\\ &+\sum_{j\neq n}\left(\partial f_{jn}/\partial\omega_{jn}\right)\left(\partial\omega_{jn}/\partial R_\varepsilon^\lambda\right)\\ &\times\langle n|x|j\rangle\langle j|y|n\rangle. \qquad (2)\end{aligned}$$

A second sum over excited states ($\sum_{j'}|j'\rangle\langle j'| = 1$) can be inserted into the expression so that

$$\begin{aligned}\left(\partial/\partial R_\varepsilon^\lambda\right)T_{\alpha\beta} = \sum_{j\neq n}\sum_{j'} f_{jn}\Big[&\left(\langle\partial n/\partial R_\varepsilon^\lambda|j'\rangle\langle j'|x|j\rangle\right.\\ &+\langle n|x|j'\rangle\langle j'|\partial j/\partial R_\varepsilon^\lambda\rangle\big)\langle j|y|n\rangle\\ &+\langle n|x|j\rangle\big(\langle\partial j/\partial R_\varepsilon^\lambda|j'\rangle\langle j'|y|n\rangle\\ &+\left.\langle j|y|j'\rangle\langle j'|\partial n/\partial R_\varepsilon^\lambda\rangle\right)\Big]\\ &+\sum_{j\neq n}\left(\partial f_{jn}/\partial\omega_{jn}\right)\left(\partial\omega_{jn}/\partial R_\varepsilon^\lambda\right)\\ &\times\langle n|x|j\rangle\langle j|y|n\rangle. \qquad (3)\end{aligned}$$

Finally, using the normalization condition ($\langle j|n\rangle = \delta_{jn}$ so that $\langle\partial j/\partial R_\varepsilon^\lambda|j\rangle = 0$, $\langle j|\partial n/\partial R_\varepsilon^\lambda\rangle = \langle\partial n/\partial R_\varepsilon^\lambda|j\rangle = -\langle\partial j/\partial R_\varepsilon^\lambda|n\rangle$) and the generalized Hellmann–Feynman theorem [13] ($\langle\partial n/\partial R_\varepsilon^\lambda|j\rangle = \omega_{jn}^{-1}\ \langle j|o|n\rangle$, $(\partial\omega_{jn}/\partial R_\varepsilon^\lambda) = \langle n|o|n\rangle - \langle j|o|j\rangle$, where $o = -\partial H/\partial R_\varepsilon^\lambda$ is the derivative of the Hamiltonian; note that symbols o comprises the indices λ and ε), the wavefunction derivatives are removed

$$\begin{aligned}\left(\partial/\partial R_\varepsilon^\lambda\right)T = \sum_{j\neq n}\sum_{j'\neq n,\,j'\neq j} f_{jn}\Big\{&\omega_{j'n}^{-1}\langle j'|o|n\rangle\\ &\times\left(\langle j'|x|j\rangle\langle j|y|n\rangle\right.\\ &+\left.\langle n|x|j\rangle\langle j|y|j'\rangle\right)\\ &+\left(f_{jn}-f_{j'n}\right)\omega_{j'j}^{-1}\langle j'|o|j\rangle\langle n|x|j'\rangle\\ &\times\langle j|y|n\rangle\Big\} - \sum_{j\neq n}\Big\{f_{jn}\omega_{jn}^{-1}\langle n|o|j\rangle\\ &\times\Big[\left(\langle n|x|n\rangle - \langle j|x|j\rangle\right)\langle j|y|n\rangle\\ &+\langle n|x|j\rangle\left(\langle n|y|n\rangle - \langle j|y|j\rangle\right)\Big]\\ &\times\left(\partial f_{jn}/\partial\omega_{jn}\right)\left(\langle n|o|n\rangle i\right.\\ &-\left.\langle j|o|j\rangle\right)\langle n|x|j\rangle\langle j|y|n\rangle\Big\}. \qquad (4)\end{aligned}$$

Here only closed shell systems and singly excited spin adapted excited states ($\Delta_{K\to J}$) [14] will be considered. As discussed before [8], multiple excitations do not explicitly enter formula (4) since x, y and o are one-particle operators ($x = \sum_i X_i$, $y = \sum_i Y_i$ and $o = \sum_i O_i$). Thus the working relation is

$$\begin{aligned}&\left(\partial/\partial R_\varepsilon^\lambda\right)T_{\alpha\beta}\\ &= 2\sum_K\sum_J\Big\{\left(\partial f_{jn}/\partial\omega_{jn}\right)\left(O^K - O^J\right)\\ &\quad\times\langle K|X|J\rangle\langle J|Y|K\rangle - f_{jn}\omega_{jn}^{-1}\langle K|O|J\rangle\\ &\quad\Big[\left(X^K - X^J\right)\langle J|Y|K\rangle + \langle K|X|J\rangle\left(Y^K - Y^J\right)\Big]\\ &\quad+\sum_{J'\neq J}\Big[f_{jn}\,\omega_{j'n}^{-1}\langle J'|O|K\rangle\left(\langle J'|X|J\rangle\langle J|Y|K\rangle\right.\\ &\quad+\left.\langle K|X|J\rangle\langle J|Y|J'\rangle\right)\\ &\quad+\left(f_{jn}-f_{j'n}\right)\omega_{j'j}^{-1}\langle J'|O|J\rangle\langle K|X|J'\rangle\langle J|Y|K\rangle\Big]\\ &\quad+\sum_{K'\neq K}\Big[f_{jn}\omega_{j'n}^{-1}\langle J|O|K'\rangle\left(\langle K'|X|K\rangle\langle J|Y|K\rangle\right.\\ &\quad+\left.\langle K|X|J\rangle\langle K|Y|K'\rangle\right)+\left(f_{jn}-f_{j'n}\right)\omega_{j'j}^{-1}\\ &\quad\times\langle K'|O|K\rangle\langle K'|X|J\rangle\langle J|Y|K\rangle\Big]\Big\}. \qquad (5)\end{aligned}$$

Letters K, K' are reserved for occupied and J, J' for virtual orbitals. It should be emphasized that while Eq. (4) is exact for exact wavefunctions, Eq. (5) is an approximation further dependent on the model of the closed shell determinant. In accord with previous works [7–9] the excitation energies were approximated as

$$\omega_{jn} = \varepsilon_J - \varepsilon_K + 2K_{JK} - J_{JK}\,, \tag{6a}$$

or

$$\omega_{jn} = \varepsilon_J - \varepsilon_K\,, \tag{6b}$$

where ε_J, ε_K are the SCF orbital energies, and K_{JK} and J_{JK} the exchange and Coulomb terms, respectively. The approximations (6a) and (6b) can be thought of as the Hartree–Fock and an independent electron limits, respectively. The latter is more desirable for DFT calculations since the Kohn–Sham energies are given by the computationally least demanding single point energy calculation, but the former lead to more accurate results in Ref. [8].

The dependence of $\boldsymbol{A}$ and $\boldsymbol{G}'$ on the coordinate system [12,15] can be used to improve the quality of the calculations in two ways. Firstly, a distributed origin gauge ensures the origin-independence of the $\boldsymbol{G}'$ tensor for any basis set used:

$$G'_{\alpha\beta}(\mathrm{SOS})\,\omega^{-1} = G'_{\alpha\beta}(0)\,\omega^{-1} + (1/2)\,\varepsilon_{\beta\gamma\delta}Y^{\lambda}_{\gamma}(\alpha^{v}_{\alpha\delta} - \alpha_{\alpha\delta})\,, \tag{7}$$

where $\boldsymbol{Y}^{\boldsymbol{\lambda}}$ is the equilibrium position of an atom λ and $\boldsymbol{G}'(0)$ was calculated according to Eq. (5). Secondly, only local parts of $\boldsymbol{G}'$ and $\boldsymbol{A}$ can be calculated by the SOS formalism and combined with $\boldsymbol{\alpha}$ obtained by CP calculations which gives the final form of the tensors and their nuclear derivatives

$$G'_{\alpha\beta}\,\omega^{-1} = G'_{\alpha\beta}(\mathrm{SOS})\,\omega^{-1} + (1/2)\,\varepsilon_{\beta\gamma\delta}Y^{\lambda}_{\gamma}\Delta\alpha_{\alpha\delta}\,, \tag{8a}$$

$$A_{\alpha,\beta\gamma} = A_{\alpha,\beta\gamma}(\mathrm{SOS}) - (3/2) \times \left[Y^{\lambda}_{\beta}\Delta\alpha_{\alpha\gamma} + Y^{\lambda}_{\gamma}\Delta\alpha_{\alpha\beta}\right] - Y^{\lambda}_{\delta}\Delta\alpha_{\alpha\delta}\,\delta_{\beta\gamma}\,, \tag{8b}$$

where $\Delta\alpha_{\alpha\delta} = \alpha_{\alpha\delta}(\mathrm{SOS}) - \alpha_{\alpha\delta}(\mathrm{CP})$.

3. Computation

The program Gaussian 94 [16] provided the SCF energies, optimized geometries, second derivatives and polarizability ($\boldsymbol{\alpha}$) derivatives while the Roa [8] program was used for the SOS calculations. Nuclear derivatives of $\boldsymbol{A}$ and $\boldsymbol{G}'$ were obtained by the CADPAC [17] program using the CHF method and a differentiation step of 0.005 bohr.

4. Results and discussion

4.1. H_2O

For the test calculations, the BPW/6-311G** optimized geometry [$O_1(0, 0, 0.1207)$, $H_2(0, 0.7582, -0.4828)$, $H_3(0, -0.7582, -0.4828)$; coordinates in Å] was used. In Table 1 diagonal polarizability components are given, calculated with the 6-311G** and AUG-cc-pVTZ (AUG) bases; using the Hartree–Fock (HF), local spin density approximation (LDA), Becke88/Perdew-Wang 91 (BPW) and Becke3LYP (B3LYP) DFT functionals as provided by the Gaussian package. The results are compared to the CP values obtained with CADPAC at the HF level. To quantify the comparison, all non-zero components of $\boldsymbol{\alpha}$ (i.e., also those not shown in the table) were fitted to the CP HF/AUG calculation ($\alpha_{\mathrm{calc.}} = a\alpha_{\mathrm{CP}}$), see the fitting and correlation coefficients at the bottom of the table. The CP calculation is least dependent on the size of the basis set ($a = 0.99$ for the 6-311G** basis), nevertheless for individual polarizability components quite large differences can be observed. The SOS results appear a rather poor approximation for the CP values, for example the best (HF/6-311G**) SOS calculation approximates the target values only by 68% on average ($a = 0.68$). Nevertheless, most of the SOS components approximately match the sign and relative magnitude of the CP results. The DFT (LDA, BPW and B3LYP) methods give qualitatively similar results, slightly worse than the HF calculation if compared to the CP standard. The B3LYP values are least dependent on the formula used for molecular

energies which is convenient since the calculations of the Coulomb and exchange terms in Eq. (6a) become unnecessary.

A significantly better performance of the SOS method can be observed for the tensors $\boldsymbol{G}'$ (static limit) and $\boldsymbol{A}$ listed in Tables 2 and 3, respectively. While the CP calculation of these tensors becomes more sensitive with respect to the size of the basis (cf. coefficient $a = 0.99$ for $\boldsymbol{\alpha}$ in Table 2 with the values of 0.77 and 0.78 for $\boldsymbol{G}'$ and $\boldsymbol{A}$ in Tables 2 and 3, respectively, for the 6-311G** basis), relative precision of the SOS calculations increases. For example, the SOS/HF/6-311G** calculation gives an even better approximation of the tensor $\boldsymbol{A}$ ($a = 0.97$ in Table 3) than the corresponding CP computation ($a = 0.78$), although the correlation coefficient remains lower.

4.2. H_2O_2

For hydrogen peroxide both the Raman and back scattering ROA (180 degrees, incident circular polarization (ICP, [12]) intensities were calculated; the B3LYP/6-31G** optimized geometry and force field were used. As apparent from Table 4 and in accord with the findings for water, the SOS method is not suitable for calculation of Raman intensities. For example, the intensity of the first mode is more than three times overestimated, if compared to the CP result. However, the ROA intensities are more consistent with respect to their relative intensity pat-

Table 1
Polarizability components for water

Basis:	6-311G** (31 bf)					AUG (105 bf)				
α [a]	HF	LDA	BPW	B3LYP	CP	HF	LDA	BPW	B3LYP	CP
1 z, xx	0.9	1.3	1.3	1.3	0.0	1.2	1.9	1.6	1.8	1.4
[b]	0.3	2.6	2.5	1.7		0.6	3.8	3.8	2.5	
2 y, xx	1.5	1.5	1.5	1.5	−0.4	4.9	7.2	7.0	6.9	1.1
[b]	0.6	2.4	2.3	1.7		2.6	12.3	12.2	8.4	
2 z, xx	−1.3	−1.4	−1.3	−1.4	0.0	−4.0	−5.9	−5.8	−5.6	−0.7
[b]	−0.6	−2.2	−2.1	−1.5		−2.1	−10.2	−10.1	−6.9	
1 z, yy	2.6	−2.4	−2.6	0.7	5.0	4.0	−0.2	−0.5	1.2	5.6
[b]	1.4	−4.0	−4.5	−0.9		3.0	−2.3	−3.0	0.7	
2 y, yy	9.1	10.6	10.8	10.5	4.9	9.8	13.4	13.3	12.7	4.7
[b]	4.4	15.0	15.1	11.3		5.7	19.9	19.8	14.9	
2 z, yy	−6.1	−7.6	−7.7	−7.4	−2.5	−5.9	−8.8	−8.6	−8.2	−2.8
[b]	−2.7	−11.3	−11.2	−8.1		−3.3	−13.7	−13.6	−9.9	
1 z, zz	−0.8	−5.8	−6.1	−4.8	6.0	−8.7	−20.4	−20.1	−18.2	5.1
[b]	0.4	−11.8	−11.8	−5.2		−3.5	−32.1	−38.6	−23.3	
2 y, zz	4.3	4.8	4.9	4.9	1.0	35.8	8.2	8.0	7.8	2.3
[b]	1.8	8.6	8.4	5.8		3.2	14.3	14.0	9.9	
a	0.68	0.23	0.20	0.38	0.99	0.64	0.22	0.20	0.34	1.00
[b]	0.38	0.21	0.15	0.29		0.49	−0.10	−0.20	0.28	
cc	0.55	0.21	0.20	0.29	0.96	0.44	0.17	0.16	0.22	1.00
[b]	0.66	0.14	0.13	0.30		0.56	0.07	0.06	0.18	

[a] $\lambda\varepsilon$, $\alpha\beta$ = the derivative of the $(\alpha\beta)$ component with respect to an ε-coordinate of the atom λ, in atomic units, only diagonal components listed.
[b] Second line for an SOS calculations with MO energies according to Eq. (6b).
a, cc = the coefficient and correlation coefficient, respectively, of a linear fit ($y = a \cdot x$) with respect to the last CP/AUG calculation; fit done for all components (also off-diagonal not shown here).

Table 2
Optical activity tensor of water

G'/ω	6-311G**					AUG				
	HF	LDA	BPW	B3LYP	CP	HF	LDA	BPW	B3LYP	CP
2*x*, *xx*	−0.1	−0.1	−0.1	−0.1	0.3	−0.2	−0.2	−0.2	−0.2	0.2
	0.0	−0.1	−0.1	−0.1		−0.1	−0.3	−0.2	−0.2	
2*x*, *yy*	−0.1	−0.2	−0.3	−0.2	−0.3	−0.3	−0.5	−0.5	−0.5	−0.2
	0.0	−0.5	−0.5	−0.2		−0.1	−0.8	−0.9	−0.5	
2*x*, *zz*	0.2	0.3	0.3	0.2	0.0	0.2	0.6	0.6	0.5	0.0
	0.1	0.4	0.4	0.2		0.2	0.9	0.9	0.6	
a	0.20	0.58	0.61	0.51	0.77	1.1	1.5	1.6	1.40	1.00
	0.14	0.92	1.0	0.48		0.5	2.3	2.4	1.6	
cc	0.28	0.48	0.48	0.46	0.96	0.76	0.75	0.75	0.76	1.00
	0.60	0.40	0.43	0.40		0.78	0.68	0.69	0.73	

Table organized analogous to Table 1.

tern and exhibit reasonable basis set dependence, except for the intensities of the modes 3 and 4, which oscillate around zero. The quality of the CP and SOS approach cannot be further compared, since experimental values are not available.

Traditionally, the dependence of Raman intensities on the frequency of the exciting light have been mostly ignored. It can be easily included in the SOS approach, at least formally, as shown in Table 5 where the spectral intensities for H_2O_2 are calcu-

Table 3
Dipole–quadrupole polarizability of water

A	6-311G**					AUG				
	HF	LDA	BPW	B3LYP	CP	HF	LDA	BPW	B3LYP	CP
1*x*, *xxx*	14.1	16.6	16.4	16.1	8.4	23.0	33.1	31.3	29.0	14.0
	5.3	27.7	27.0	16.9		13.1	48.9	46.4	32.0	
2*x*, *xxx*	0	−0.2	−0.2	−0.1	−0,4	2.3	3.1	3.1	3.0	0.8
	0	−0.3	−0.4	−0.2		1.1	4.8	4.7	3.5	
1*y*, *yyy*	23.0	32.7	33.5	30.4	−3.2	36.7	53.8	53.3	49.4	0.2
	10.6	46.5	46.9	31.5		20.8	77.0	76.6	55.8	
2*y*, *yyy*	8.0	9.3	9.5	9.3	9.2	8.5	11.5	11.5	10.9	9.3
	4.2	12.9	13.0	9.9		5.2	16.1	16.2	12.5	
1*z*, *zzz*	10.5	12.1	12.0	11.3	6.2	36.1	55.9	53.6	50.6	8.4
	5.5	18.3	17.7	13.4		21.4	87.7	83.4	60.2	
2*z*, *zzz*	2.0	2.0	2.0	1.9	2.6	6.1	8.6	8.3	8.1	4.4
	1.2	2.5	2.4	2.1		3.5	14.0	13.3	9.8	
a	0.97	1.1	1.1	1.1	0.78	2.0	2.9	2.8	2.6	1.00
	0.48	1.7	1.7	1.2		1.20	4.3	4.1	3.0	
cc	0.57	0.49	0.49	0.51	0.94	0.69	0.66	0.66	0.66	1.00
	0.61	0.48	0.48	0.51		0.70	0.63	0.63	0.65	

Table organized in an analogy to Tables 1 and 2.

lated for three frequencies. Although the changes are minor given the expected error, the dependence can be crucial for other systems closer to the resonance range and would certainly deserve a more detailed analysis in the future.

4.3. α-Pinene and pinane

In Fig. 1 ROA spectra (ICP, back scattering) for α-pinene and trans-pinane are plotted as calculated by the SOS and CP methods and compared to the experiment from Ref. [1]. In the same reference, details about the CP calculation and the mode assignment can be also found. For all calculations the B3LYP/6-31G** level of approximation was used, only the numerical differentiation for the CP method had to be done using the HF/6-31G model because of computer limitations. A general agreement between the calculated and experimental spectra can be observed in Fig. 1 for both molecules, yet several bands are calculated with incorrect signs. The most obvious miscalculations are marked by '×'. For α-pinene, both the CP and SOS methods fail most often in the region about 800–1000 cm^{-1} (complicated ring and C–H bending deformations). Here the SOS method gives a rather unrealistic representation of the experimental spectrum. In the C–H bend (experimentally about 1450 cm^{-1}) and ring breathing (500–750 cm^{-1}) regions both methods reproduce well the observed sign pattern. Relative intensities are slightly better matched with the CP calcula-

Table 5
The dependence of spectral intensities on the excitation wavelength for H_2O_2

Mode	λ (nm)		
	414	514	614
Raman:			
1	342	329	321
2	75	72	71
3	98	95	93
4	6	6	6
5	523	516	513
6	4	4	4
ROA_{180}:			
1	837	794	771
2	−265	−252	−246
3	−144	−139	−136
4	122	119	117
5	351	333	323
6	−30	−27	−26

Table 4
Calculated Raman and ROA intensities for H_2O_2 [a]

		6-31G (22 bf)			6-31G** (40 bf)			AUG (160 bf)		
	ω	HF	B3LYP	CP	HF	B3LYP	CP	HF	B3LYP	CP
Raman:										
1	3644	349	306	116	328	318	99	347	690	105
2	3643	89	74	56	72	70	43	27	63	28
3	1383	50	41	9	94	92	7	154	244	5
4	1279	0	0	4	6	5	2	11	15	1
5	897	151	310	39	516	701	33	830	1642	41
6	370	1	2	12	4	6	7	8	22	2
ROA:										
1		534	430	518	506	423	465	210	249	322
2		−134	−150	−390	−136	−141	−354	−104	−121	−256
3		−40	−41	6	−24	−21	2	3	9	1
4		12	43	−18	16	43	−12	−7	15	−6
5		43	98	13	35	59	9	15	59	9
6		−75	−84	−98	−52	−45	−62	−18	−6	−20

[a] Frequencies (B3LYP/6-31G**) in cm^{-1}, intensities in atomic units, ROA ($I_R - I_L$, ICP back scattering) multiplied by 1000.

tion (only calculated spectra are plotted with the same scale). For trans-pinane the CP and SOS spectra differ less than for α-pinane, if judged from a visual comparison and occasional disagreements can be observed for both methods rather outside the 'fingerprint' region 800–1000 cm^{-1}. For most of the transitions the SOS method yields slightly bigger absolute intensities than CP, thus exaggerating the errors.

To compare calculational times, a trial calculation on α-pinane was performed on one SGI processor (190 MHz) where 2.5 days of the CPU time were needed for estimation of the second derivatives (B3LYP/6-31G**). The CP differentiation (HF/6-31G) took an additional 2.3 days, while the SOS calculation at the same level finished within 5.5 h. The CPU times are obviously dependent on the actual implementation, for example, 5 h of the SOS calculation were spent on the re-calculation of the two-electron integrals needed in Eq. (6a). Note, however, that the SOS method is in principle less demanding on computer resources since the 'coupled-perturbed' terms are realised via inexpensive one-electron integrals. For example, no additional two-electron integrals are needed if compared with a single point energy calculation. Current implementation of the method also requires significantly less disk space (7 Mbytes) if compared to the CP approach (209 Mbytes). Obviously, more sophisticated SOS methods based on the expression (4) would require more computer resources than the closed shell approximation pursued here. However, the CP approach could become faster when an analytical expression of the tensor derivatives is found and implemented.

4.4. R-methyloxirane

For R-methyloxirane the SOS method (at the BPW/6-31G** level) is compared to a 'benchmark' calculation with an MP2 force field and a gauge invariant atomic orbital (GIAO, aug-cc-pVDZ) basis [18]. The frequencies and ROA circular intensity differences for right-angle scattering are given in Table 6. The SOS method gives signs of 7 modes (of the total of 18) wrong and its performance, especially for the lower frequency modes, is quite poor. Even the most advanced CP/GIAO method predicts

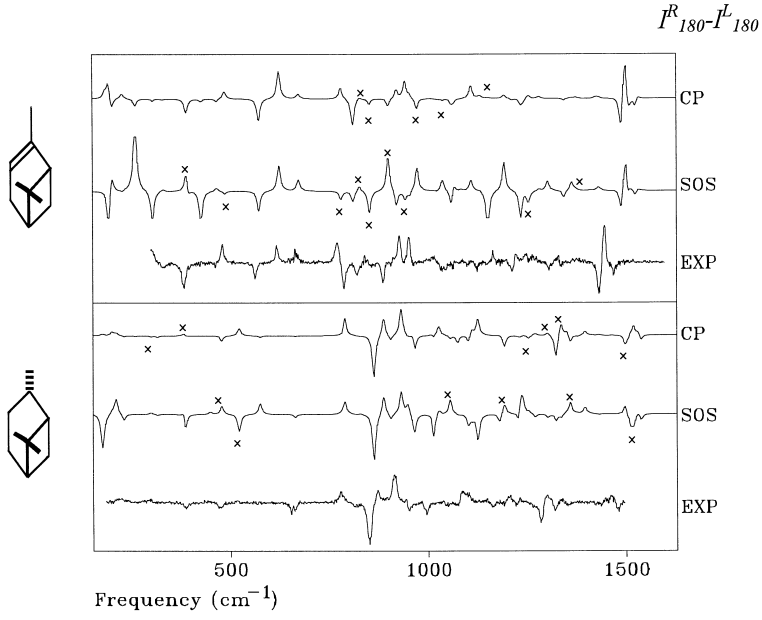

Fig. 1. Calculated and experimental ROA spectra for (1S)-(−)-α-pinene (top) and (−)-trans-pinane (bottom). Raw back-scattering intensities plotted, theoretical spectra on the same scale; see Ref. [1] for details on the experiment. Calculated bands with wrong signs are marked by '×'.

Table 6
Comparison of the SOS and GIAO calculations of ROA intensities for R-methyloxirane (the frequencies are in cm^{-1})

ω_{MP2} [a]	ω_{BPW}	ω_{exp} [a]	Δ_{90}(SOS)	Δ_{90}(GIAO)[a]	Δ_{90}(exp)[a]
1659	1504	1498	3.6	6.2	1.0
11595	1471	1460	−1.2	−7.2	−2.7
1578	1456	1450	−2.3	2.2	0.8
1561	1409	1403	4.5	2.6	3.1
1504	1371	1365	2.4	−1.8	–
1392	1266	1262	2.9	−1.0	–
1291	1153	1163	8.9	8.4	4.0
1274	1130	1140	1.9	0.5	−3.3
1158	1113	1135	11.5	−7.3	−3.8
1117	1098	1101	−18.0	−2.7	1.2
1123	1010	1020	−10.5	−1.3	−5.1
1059	955	946	−24.8	−2.2	8.3
973	881	892	6.0	2.6	4.6
929	834	824	−0.9	1.5	1.5
844	761	742	−7.0	0.8	−3.1
439	398	419	48.4	0.8	5
394	353	360	−39.7	2.9	2.5
225	211	200	29.8	2.1	+

[a] Ref. [18].
Δ_{90} is the dimensionless circular intensity difference for right-angle scattering.

the signs of four modes incorrectly thus revealing the limitations of the theoretical modelling of ROA. Fortunately, the electronic structure of the oxirane ring is rather exceptional and a better performance of both the SOS and CP methods was observed for other systems. In the author's opinion, the implementation of GIAOs is not crucial for the modelling of the vibrational optical activity, since the origin-independence of the VCD and ROA intensities can be insured by the distributed origin gauge, unlike for the modelling of NMR spectra, for example.

5. Conclusions

The simulation of Raman optical activity based on the sum-over-states expansion can be used as an alternative to the coupled-perturbed/finite difference methods used previously. While the former approach is computationally substantially cheaper and thus suitable for bigger systems the latter exhibits better numerical stability and convergence behaviour.

Acknowledgements

The work was supported by the Grant Agency of the Czech Republic (grant 203/97/P002).

References

[1] P. Bouř, V. Baumruk, J. Hanzlíková, Collect. Czech. Chem. Commun. 62 (1997) 1384.
[2] C.N. Tam, P. Bouř, T.A. Keiderling, J. Am. Chem. Soc. 118 (1996) 10285.
[3] L.D. Barron, L. Hecht, Adv. Spectrosc. Biomol. Spectrosc., Part B 21 (1993) 235.
[4] G. Wilson, L. Hecht, L.D. Barron, Biochemistry 35 (1996) 12518.
[5] A.F. Bell, L. Hecht, L.D. Barron, J. Am. Chem. Soc. 119 (1997) 6006.
[6] A.F. Bell, L. Hecht, L.D. Barron, J. Mol. Struct. 349 (1995) 401.
[7] V.G. Malkin, O.L. Malkina, L.A. Eriksson, D.R. Salahub, in: J.M. Seminario, P. Politzer (Eds.), Modern Density Functional Theory, Elsevier, Amsterdam, 1995, p.273.
[8] P. Bouř, Chem. Phys. Lett. 265 (1997) 65.
[9] P. Bouř, J. McCann, H. Wieser, J. Phys. Chem. A 101 (1997) 9783.
[10] P. Lazzeretti, M. Defranceschi, G. Berthier, Advances in Quantum Chemistry, vol. 26, Academic Press, San Diego, CA, 1995, p.2.
[11] P.L. Polavarapu, P.K. Bose, L. Hecht, L.D. Barron, J. Phys. Chem. 97 (1993) 1781.
[12] L.D. Barron, Molecular Light Scattering and Optical Activity, Cambridge University Press, Cambridge, 1982.
[13] R.G. Parr, W. Yang, Density-Functional Theory of Atoms and Molecules, Oxford University Press, New York, 1989.
[14] A. Szabo, N.S. Ostlund, Modern Quantum Chemistry, McGraw-Hill, New York, 1989.
[15] P. Bouř, J. Sopková, L. Bednárová, P. Maloň, T.A. Keiderling, J. Comput. Chem. 18 (1997) 646.
[16] M.J. Frisch, G.W. Trucks, H.B. Schlegel, P.M.W. Gill, B.G. Johnson, M.A. Robb, J.R. Cheeseman, T. Keith, G.A. Petersson, J.A. Montgomery, K. Raghavachari, M.A. Al-Laham, V.G. Zakrzewski, J.V. Ortiz, J.B. Foresman, J. Cioslowski, B.B. Stefanov, A. Nanayakkara, M. Challacombe, C.Y. Peng, P.Y. Ayala, W. Chen, M.W. Wong, J.L. Andres, E.S. Replogle, R. Gomperts, R.L. Martin, D.J. Fox, J.S. Binkley, D.J. DeFrees, J. Baker, J.P. Stewart, M. Head-Gordon, C. Gonzalez, J.A. Pople, Gaussian 94, Revision E.2, Gaussian, Inc., Pittsburg, PA, 1995.
[17] R.D. Amos, J.E. Rice, CADPAC: The Cambridge Analytic Derivatives Package, issue 5.0, Cambridge, 1990.
[18] T. Helgaker, K. Ruud, K.L. Bak, P. Jørgensen, J. Olsen, Faraday Discuss. 99 (1994) 165.